

Temperature dependence of the electrical, mechanical and electromechanical properties of high sensitivity novel piezoceramics

M. ALGUERÓ, B. JIMÉNEZ, C. ALEMANY, L. PARDO
Instituto de Ciencia de Materiales de Madrid, CSIC. Cantoblanco 28049, Madrid. Spain

The temperature dependence of the ϵ_{33}^T dielectric permittivity and losses of piezoelectric Mn doped $0.65\text{Pb}(\text{Mg}_{1/3}\text{Nb}_{2/3})\text{O}_3$ - 0.35PbTiO_3 ceramics has been measured up to 350°C at frequencies between 1 and 100 kHz by impedance spectroscopy. The temperature dependence of the low frequency Young's modulus and mechanical losses of the ceramics has been measured in the same temperature range by dynamic mechanical analysis in three points bending configuration. Complex ϵ_{33}^T , s_{11}^E compliance and d_{31} piezoelectric coefficients have been obtained from radial piezoelectric resonances at temperatures up to 90°C (before depolarisation) by an automatic iterative method. All the measurements reflect the occurrence of the ferroelectric rhombohedral to ferroelectric tetragonal phase transition, which is thought to be responsible of the high electromechanical response of the PMN-PT system, and allow describing some of its characteristics for the investigated ceramics.

Keywords: Piezoelectric ceramics, Relaxor ferroelectrics, PMN-PT, Mechanical properties, Electromechanical Properties

Dependencia con la temperatura de las propiedades eléctricas, mecánicas y electromecánicas de nuevas piezocerámicas de alta sensibilidad

Se ha medido por espectroscopía de impedancias la dependencia con la temperatura hasta 350°C de la permitividad y las pérdidas dieléctricas, ϵ_{33}^T y $\tan \delta$, de cerámicas piezoeléctricas de $0.65\text{Pb}(\text{Mg}_{1/3}\text{Nb}_{2/3})\text{O}_3$ - 0.35PbTiO_3 dopadas con Mn a frecuencias entre 1 y 100 kHz. Se ha medido por análisis mecánico dinámico en la configuración de flexión por tres puntos la dependencia con la temperatura en el mismo rango del módulo de Young y las pérdidas mecánicas de baja frecuencia de las cerámicas. Se han obtenido por un método automático iterativo los coeficientes del material ϵ_{33}^T , módulo elástico s_{11}^E y coeficiente piezoeléctrico d_{31} en forma compleja a partir de resonancias radiales piezoeléctricas a temperaturas entre ambiente y 90°C (antes de la despolarización). Todas las medidas reflejan la existencia de la transición de la fase ferroeléctrica con estructura romboédrica a la fase ferroeléctrica con estructura tetragonal, que se cree responsable de la alta respuesta electromecánica del sistema PMN-PT, y permiten describir algunas de sus características para las cerámicas concretas investigadas.

Palabras claves: Cerámicas Piezoeléctricas, Ferroeléctricos Relaxores, PMN-PT, Propiedades Mecánicas, Propiedades Electromecánicas

1. INTRODUCTION

The discovery in 1997 of ultrahigh piezoelectricity ($d_{33} > 2000$ pC N⁻¹) and electric field induced strain (>1.5%) for rhombohedral structure $\text{Pb}(\text{Zn}_{1/3}\text{Nb}_{2/3})\text{O}_3$ - PbTiO_3 (PZN-PT) and $\text{Pb}(\text{Mg}_{1/3}\text{Nb}_{2/3})\text{O}_3$ - PbTiO_3 (PMN-PT) single crystals with compositions close to the rhombohedral-tetragonal morphotropic phase boundary (MPB) (1) has aroused a renewed interest in these relaxor-ferroelectric solid solutions. The ultrahigh electromechanical response is observed along the <001> direction of the pseudocubic structure in spite of the spontaneous polarisation being along the <111> direction. This effect was related to the occurrence of a rhombohedral to tetragonal phase transition (with polarisation rotation) under the electric field (2). A recent high energy X-ray diffraction study on 0.92PZN-0.08PT crystals has shown that the initial rhombohedral phase first transforms into a monoclinic structure (3). A low temperature monoclinic phase has been found by neutron diffraction in 0.91PZN-0.09PT and 0.65PMN-0.35PT powders (4).

Work on ceramics of these solid solutions has mainly been focused on the low PT content relaxor edge of the PMN-PT system (PMN and 0.9PMN-0.1PT), because of the high dielectric permittivity and electrostrictive effect (5). Piezoelectric higher PT content compositions have been scarcely studied, in spite of presenting at the MPB, ~0.65PMN-0.35PT (6-8), values of the d_{33} piezoelectric coefficient comparable or even higher (720 pC N⁻¹) than the best lead titanate

zirconate (PZT) ceramics (8). This MPB curves towards the PMN edge with temperature. Therefore, ceramics with compositions around the MPB with rhombohedral structure or phase coexistence undergo the rhombohedral to tetragonal transformation on heating. We present here a study on the temperature dependence of the electrical, mechanical and electromechanical properties of 0.65PMN-0.35PT piezoceramics. It was intended to evaluate two non-standard techniques: complex dynamic mechanical analysis in three points bending configuration and an automatic iterative method for determining the complex coefficients involved in a piezoelectric resonance as a means of studying the rhombohedral to tetragonal phase transition for PMN-PT ceramics.

2. MATERIALS AND EXPERIMENTAL METHODS

Poled Ag electroded Mn doped $0.65\text{Pb}(\text{Mg}_{1/3}\text{Nb}_{2/3})\text{O}_3$ - 0.35PbTiO_3 ceramic discs and plates were received from Thales Research and Technologies (France). Mn doping was used to increase the dielectric strength of the ceramics (7). Bragg-Brentano X-ray diffraction patterns (Siemens D500 powder diffractometer with Cu k_α radiation) of the ceramics showed that they were single phase perovskite structure (see Figure 1). The patterns also suggested coexistence of the

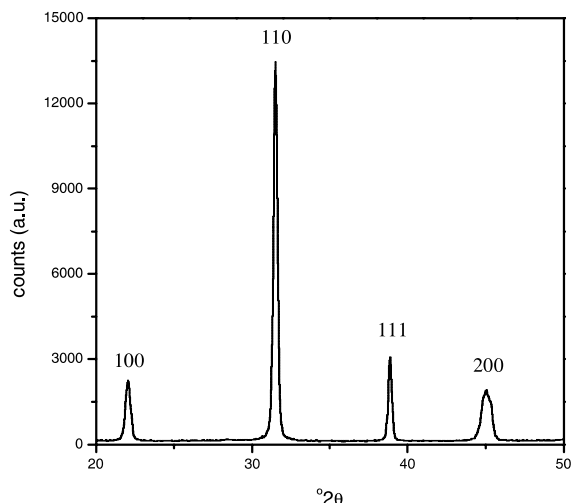


Figure 1. X-ray diffraction pattern of a Mn doped 0.65PMN-0.35PT ceramic.

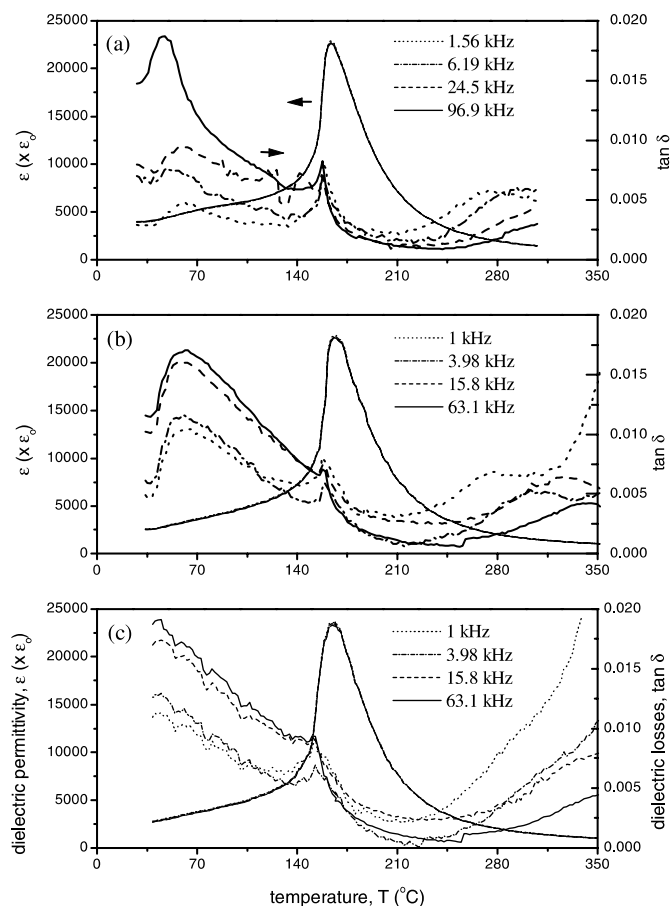


Figure 2. Dielectric permittivity and losses of a Mn doped 0.65PMN-0.35PT ceramic, (a) first run, heating (poled), (b) second run, heating (unpoled), (c) second run, cooling.

rhombohedral and tetragonal structures (note the lack of tetragonal splitting and significant broadening of the 200 diffraction peak). Ceramics presented a residual porosity of 0.33% (as measured by quantitative image analysis, IMCO10-KAT386, Kontron Elektronik, on polished surfaces). A fine grain microstructure with a grain size of $1.7 \pm 0.4 \mu\text{m}$ (equivalent diameter average and standard deviation, also measured by quantitative image analysis) was revealed by thermal etching and quenching from 900°C .

The temperature dependence of the dielectric permittivity and

dielectric losses was recorded with a HP 4194A impedance gain phase analyser from room temperature (RT) to 350°C at frequencies between 1 and 100 kHz.

The temperature dependence of the low frequency Young's modulus and mechanical losses was measured with a DMA7 Perkin Elmer (three points bending configuration (TPB)), also from RT to 350°C , at 9 Hz. Thickness poled TPB samples (12 mm long, 2 mm wide and 0.5 mm thick) for these measurements were machined from the received plates after polishing the sintered Ag electrodes off. Details of the procedure can be found in (9).

The piezoelectric radial resonance of poled discs (12 mm ϕ) was recorded with a HP4192A LF impedance analyser at increasing temperatures from RT up to 90°C (before thermal depolarisation), and the material coefficients relevant to the radial mode (ϵ_{33}^T permittivity, s_{11}^E and s_{12}^E compliances and d_{31} piezoelectric coefficient) were obtained in complex form by an automatic method as a function of temperature (10). This method rests on solving (by an iterative numerical procedure) the set of non-linear equations that result when complex experimental impedance or admittance values are introduced into the known piezoelectric resonance analytical solution. Data at as many frequencies as unknown coefficients are necessary for a given resonance, yet an additional frequency is measured for numerical convenience. Once the coefficients have been obtained, the resonance profiles are reconstructed by using this analytical solution and compared with the experimental ones. This comparison is a test of the reliability of the coefficients.

3. RESULTS AND DISCUSSION

The temperature dependence of the relative dielectric permittivity and dielectric losses is shown in Figure 2 at four frequencies within the 1-100 kHz range. The permittivity did not show any frequency dispersion, indicating that the disorder/local order giving place to the relaxor behaviour characteristic of PMN-PT with low PT content has fully disappeared at 0.35PT (11). The first heating (disc still poled), second heating (unpoled) and second cooling (unpoled) runs are shown in Figures 2a, b and c, respectively. Two dielectric anomalies were observed. A change of slope was found at $\sim 75^\circ\text{C}$ on heating, more pronounced for the first run (poled) than for the second (unpoled). The dielectric losses showed an associated, rather broad maximum at $\sim 60^\circ\text{C}$, that further broadened for the second run. This first anomaly has been related to the ferroelectric rhombohedral to ferroelectric tetragonal phase transition (6,7). On cooling, this anomaly was clearly shifted $\sim 30^\circ\text{C}$ to lower temperatures, indicating a strong thermal hysteresis in the transition. A second dielectric anomaly related to the ferroelectric (tetragonal) to paraelectric (cubic) phase transition occurred at $\sim 165^\circ\text{C}$. Thermal hysteresis was not observed. Additionally, a highly dispersive dielectric loss maximum was found at higher temperatures, $>250^\circ\text{C}$, that could be related to the dynamics of dipolar defects (12, 13).

The temperature dependence of the Young's modulus and mechanical losses at 9 Hz is shown in Figure 3. The first heating (bar still poled), second heating (unpoled) and second cooling (unpoled) runs are shown in Figures 3a, b and c. Therefore, a direct comparison between Figures 2 and 3 can be done. Two elastic anomalies were observed. A first minimum of the Young's modulus was observed at $\sim 60^\circ\text{C}$, which had associated a maximum in the mechanical losses, broader for the second run. The anomaly also shifted to room temperature on cooling. This anomaly, as its dielectric counterpart, is most probably related to the rhombohedral to tetragonal phase transition. A second elastic anomaly related to the ferroelectric to paraelectric phase transition occurred at $167\text{-}170^\circ\text{C}$ on heating, and at 158°C on cooling. Note the huge stiffening and vanishing losses after the transition linked to

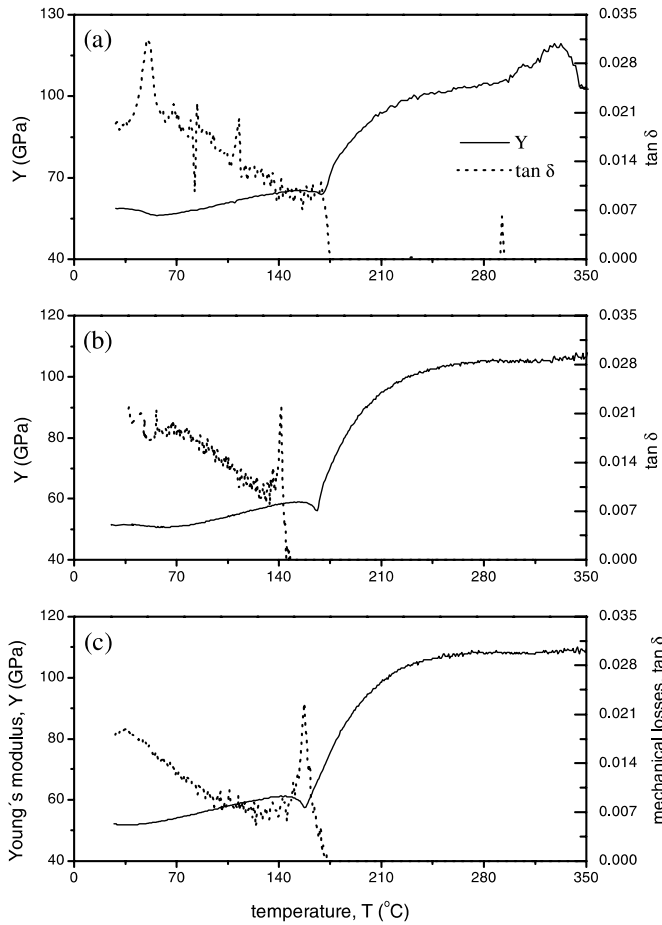


Figure 3. 9 Hz Young's modulus and mechanical losses of a Mn doped 0.65PMN-0.35PT ceramic, (a) first run, heating (poled), (b) second run, heating (unpoled), (c) second run, cooling.

the disappearance of the ferroelectric/ferroelastic domains. Thermal hysteresis was not observed for the dielectric anomaly. Therefore, the thermal hysteresis for the mechanical feature is likely an artefact of the sample preparation. TPB bars were cold machined (to avoid depolarisation) from square plates, and extensive stresses were most probably introduced, which can affect the transition. As a matter of fact, the Young's modulus at high temperature (>300°C) showed a broad maximum on the first heating, which might be related to partial stress relaxation through defects movements (13).

A typical room temperature radial piezoelectric resonance is shown in Figure 4. Similarly, very clean resonances were obtained at all temperatures up to 90°C, which indicated the homogeneity of the ceramic discs. An extremely good agreement ($R^2=0.999$) was obtained between the experimental and reconstructed profiles all across the temperature range. Obtained coefficients are given in Figure 5. The relative dielectric permittivity and losses (at the resonance frequency, ~192 kHz) are shown in Figure 5a. These should be directly comparable with the dielectric parameters obtained by standard impedance spectroscopy (Figure 2a), and the agreement is very good indeed. The s_{11}^E compliance and mechanical losses are shown in Figure 5b. This measurement is also comparable with the complex dynamic mechanical analysis (DMA) results for the poled bar (Figure 3a) with some cautions. DMA provides the Young's modulus, Y , i.e. a stiffness coefficient, and the piezoelectric resonance a compliance, though both in the transverse direction to the polarisation. Therefore the latter has a maximum where the former had a minimum. Measuring frequencies are also different, 9 Hz versus 192 kHz. Differences in frequency should

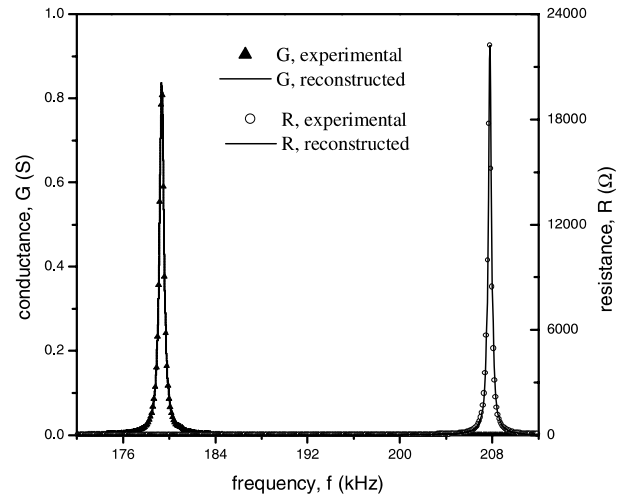


Figure 4. Room temperature radial piezoelectric resonance of a Mn doped 0.65PMN-0.35PT ceramic disc (12 mm ϕ).

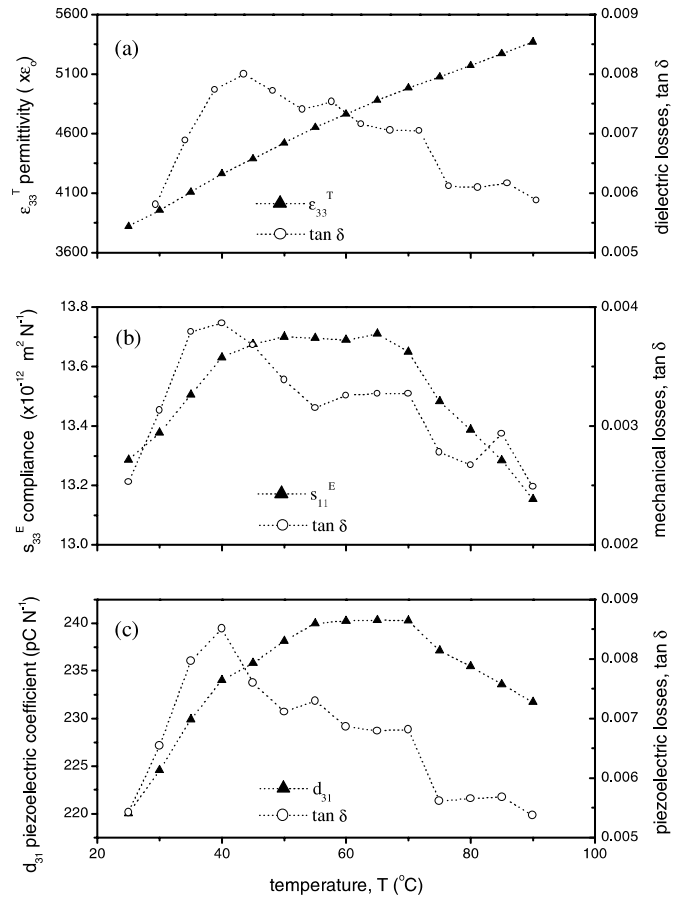


Figure 5. Complex material coefficients of a Mn doped 0.65PMN-0.35PT ceramic obtained from the radial piezoelectric resonance, (a) dielectric permittivity, (b) transverse elastic compliance, (c) transverse piezoelectric coefficient.

not affect the phase transition, and so, analogous behaviours were found for Y and s_{11}^E . The loss mechanism is basically ferroelectric/ferroelastic domain wall movements, which are known to be active all across this frequency range. Finally, the d_{31} transverse piezoelectric coefficient is shown in Figure 5c. A broad maximum between 50-70°C was found, which must be linked to the rhombohedral to tetragonal phase transition. Piezoelectric losses, also related to ferroelectric/ferroelastic domain wall movements (14), also showed a maximum, indicating an increase of the walls activity around the transition

4. CONCLUSIONS

It has been shown that complex dynamic mechanical analysis in three points bending configuration, and the automatic iterative method for the determination of complex material coefficient from piezoelectric resonances are suitable methods for studying the rhombohedral to tetragonal phase transition for PMN-PT ceramics. This transition has been characterised for Mn doped 0.65PMN-0.35PT ceramics with phase coexistence, and showed to occur in a broad temperature range between 50 and 70°C with a strong thermal hysteresis on a heating/cooling cycle. This transition has associated a maximum of the piezoelectric coefficient and a significant enhancement of the ferroelectric/ferroelastic domain wall activity. The low frequency Young's modulus also reflects the ferroelectric to paraelectric phase transition, which for the ceramics investigated occurs at 165°C. A strong thermal hysteresis appears for the three points bending specimens, most probably related to internal stresses introduced during cold machining.

ACKNOWLEDGEMENTS

This research is being supported by the European Commission through a Growth Project ("PIRAMID", ref. G5RD-CT-2001-00456) and by the Spanish MCyT through the "Acción Especial" MAT2001-4819-E and a "Ramón y Cajal" contract. Authors are very grateful to Dr. Mai Pham Thi, from Thales Research and Technologies (France), for kindly providing the ceramic samples.

BIBLIOTECA

1. E. Park and T.R. Shrout. "Ultra-high strain and piezoelectric behavior in relaxor based ferroelectric single crystals". *J. Appl. Phys.* **82**, 1804-1811 (1997).
2. M.K. Durbin, E.W. Jacobs, J.C. Hicks and S.E. Park. "In situ X-ray diffraction study of an electric field induced phase transition in the single crystal relaxor ferroelectric 92% Pb(Zn_{1/3}Nb_{2/3})O₃-8%PbTiO₃". *Appl. Phys. Lett.* **74**, 2848-2850 (1999).
3. B. Noheda, D.E. Cox, G. Shirane, S.E. Park, L.E. Cross and Z. Zhong. "Polarization rotation via a monoclinic phase in the piezoelectric 92%PbZn_{1/3}Nb_{2/3}O₃-8%PbTiO₃". *Phys. Rev. Lett.* **86**, 3891-3894 (2001).
4. J.M. Kiat, Y. Uesu, B. Dkhil, M. Matsuda, C. Malibert and G. Calvarin. "Monoclinic structure of unpoled morphotropic high piezoelectric PMN-PT and PZN-PT compounds". *Phys. Rev. B.* **65**, 064106-1-4 (2002).
5. S.L. Swartz, T.R. Shrout, W.A. Schulze and L.E. Cross. "Dielectric properties of lead magnesium niobate ceramics". *J. Am. Ceram. Soc.* **67**, 311-315 (1984).
6. S.W. Choi, T.R. Shrout, S.J. Jang and A.S. Bhalla. "Dielectric and pyroelectric properties in the Pb(Mg_{1/3}Nb_{2/3})O₃-PbTiO₃ system". *Ferroelectr.* **100**, 29-38 (1989).
7. O. Noblanc, P. Gaucher and G. Calvarin. "Structural and dielectric studies of Pb(Mg_{1/3}Nb_{2/3})O₃-PbTiO₃ ferroelectric solid solutions around the morphotropic boundary". *J. Appl. Phys.* **79**, 3291-4297 (1996).
8. J. Kelly, M. Leonard, C. Tantigate and A. Safari. "Effect of composition on the electromechanical properties of (1-x)Pb(Mg_{1/3}Nb_{2/3})O₃-xPbTiO₃ ceramics". *J. Am. Ceram. Soc.* **80**, 957-964 (1997).
9. B. Jiménez and J.M. Vicente. "Oxygen defects and low frequency mechanical relaxation in Pb-Ca and Pb-Sm titanates". *J. Phys. D: Appl. Phys.* **31**, 446-452 (1998).
10. C. Alemany, A.M. González, L. Pardo, B. Jiménez, F. Carmona and J. Mendiola. "Automatic determination of complex constants of piezoelectric lossy materials in the radial mode". *J. Phys. D: Appl. Phys.* **28**, 945-956 (1995).
11. D. Viehland, M.C. Kim, Z. Xu and J.F. Li. "Long-term present tweedlike precursors and paraelectric clusters in ferroelectrics containing strong quenched randomness". *Appl. Phys. Lett.* **67**, 2471-2473 (1995).
12. H.S. Shulman, D. Damjanovic and N. Setter. "Niobium doping and dielectric anomalies in bismuth titanate". *J. Am. Ceram. Soc.* **83**, 528-532 (2000).
13. B. Jiménez, R. Jiménez, A. Castro, P. Millán and L. Pardo. "Dielectric and mechanoelastic relaxations due to point defects in layered bismuth titanate ceramics". *J. Phys.: Condens. Matter* **13**, 7315-7326 (2001).
14. G. Robert, D. Damjanovic and N. Setter. "Piezoelectric hysteresis analysis and loss separation". *J. Appl. Phys.* **90**, 4668-4675 (2001).

Recibido: 1.2.03

Aceptado: 30.11.03

